JOURNAL OF CATALYSIS 46, 143–150 (1977)

Adsorption, Reactivity and Surface Structural Chemistry of Hydrogen Cyanide on Pt(110)

M. E. BRIDGE AND R. M. LAMBERT

Department of Physical Chemistry, University of Cambridge, Cambridge CB2 1EP, England

Received May 13, 1976

The adsorption, desorption, surface structural chemistry, and reactivity of HCN adsorption layers on Pt(110) have been studied by LEED and thermal desorption mass spectrometry. HCN adsorbs at 300 K via a mobile precursor state, and induces a $(1 \times 2) \rightarrow (1 \times 1)$ change in the periodicity of the clean reconstructed Pt(110) surface. Desorption occurs yielding H_2, HCN and C_2N_2 in comparable quantities, and the observed behavior is accounted for in terms of associative desorption from a fully dissociated layer of H and CN species. A simple model is developed using lattice statistics which gives a fairly good account of the observed desorption spectra and their coverage dependence, both as regards peak temperature shifts and product distribution. Comparison of the observed and calculated spectra for C_2N_2 leads to the following conclusions: (i) the initial sticking probability of HCN is of the order of unity; (ii) H and CN occupy different kinds of adsorption site; (iii) CN itself is a "two-site" adsorbate at 300 K. $c(2 \times 4)$ and (1×1) LEED patterns due to adsorbed CN are observed which are consistent with this view; under certain conditions a more compressed, poorly ordered $|1\frac{2}{3}, \bar{1}\frac{2}{3}|$ structure is also observed.

INTRODUCTION

The surface chemistry of HCN on Pt is of interest in relation to both the synthesis of HCN itself by the catalytic oxidation of CH_4 over Pt (*1*), and in the use of HCN as a reagent in the oxycyanation of olefins over metals of the Pt group (*2*). Furthermore, fundamental studies of the chemisorbed CN radical on Pt are a logical extension of our earlier work (*3–6*) on the closely related species CO and NO. The Pt(110) surface is reconstructed (1×2) and a number of adsorbates have been found to induce the $(1 \times 2) \rightarrow (1 \times 1)$ transformation, even at 300 K. This periodicity change produces unusual effects in the adsorption kinetics of linear polyatomic molecules such as C_2N_2 and C_3O_2, but no such effects are observed with CO and NO. HCN lies in the middle of this series of molecules.

EXPERIMENTAL METHODS

Experiments were carried out in a stainless steel ultrahigh vacuum chamber, whose contents and mode of operation have been described in detail elsewhere (*4*). The chamber was fitted with a standard 3-grid retarding field analyzer for LEED and Auger spectroscopy, and a quadrupole mass spectrometer for gas analysis and thermal desorption measurements. Base pressures of $< 5 \times 10^{-11}$ Torr (1 Torr = 133.3 $N\,m^{-2}$) were routinely obtainable. The Pt(110) specimen was cut from an ingot of 99.999% purity, followed by mechanical and chemical polishing as previously described (*6*). Hydrogen cyanide of >98% purity was prepared by the reaction of H_2SO_4 with KCN, followed by liquefaction, fractionation, and dehydration of the HCN so formed. The Pt(110) surface was cleaned

ISSN 0021-9517

by an iterative sequence of (i) heating in oxygen (700 K at 10^{-6} Torr), (ii) Ar^+ bombardment (10^{-4} A m^{-2} at 490 eV), (iii) annealing *in vacuo* at 1200 K, until the Auger spectrum showed Pt transitions only.

RESULTS

A. Adsorption–Desorption Kinetics and Surface Reactivity

Adsorption of HCN at 300 K followed by thermal desorption using a linear heating rate of 13 K s^{-1} showed that the adlayer desorbs as a mixture of HCN (27 amu), C_2N_2 (56 amu), and H_2 (2 amu); 26 amu (CN^+) desorption spectra were also obtained as a monitor of the total yield of (HCN + C_2N_2). Typical desorption spectra are shown in Fig. 1a–f. The H_2 and HCN spectra always show a single peak (Fig. 1a and b); on the other hand, the C_2N_2 spectra show a single peak at low coverage (Fig. 1c) but two peaks at high coverage (Fig. 1d). We shall denote these as β_1 and β_2. The H_2 and HCN peak temperatures were essentially independent of surface coverage, indicating an apparent kinetic order of unity for the desorption of both species. On the other hand, the β_1 and β_2 C_2N_2 peak temperatures showed a pronounced coverage dependence [identical with that found (*8*) in our studies of C_2N_2 adsorption] indicating a more complex kinetic behavior. Clearly, any reaction model for the adlayer must be required to explain these features. A 52 amu desorption spectrum taken from a surface saturated by adsorption of cyanogen is shown for reference purposes in Fig. 1f. Qualitatively similar spectra resulting from C_2N_2 adsorption on Pt(100) have been observed by Netzer (*17*, *18*). The noteworthy feature here is that, in addition to the β_1, β_2 peaks which are identical with those from HCN adlayers, a low temperature peak (α) also appears; this α peak was never observed in the 52 amu spectra obtained from adlayers obtained by dosing with HCN. Of the three peaks in the 26 amu spectrum (Fig. 1e), those at ~700 and ~920 K are the contribution from desorbing C_2N_2, while that at ~420 K is due to HCN.

Since the experimental conditions were such that (*5*) the desorption spectra provide a reliable relative measure of amounts of material desorbing, such spectra may be used to determine the variation with coverage of the desorption yields of H_2, HCN, and C_2N_2. The H_2 spectra themselves could not be used quantitatively, because control

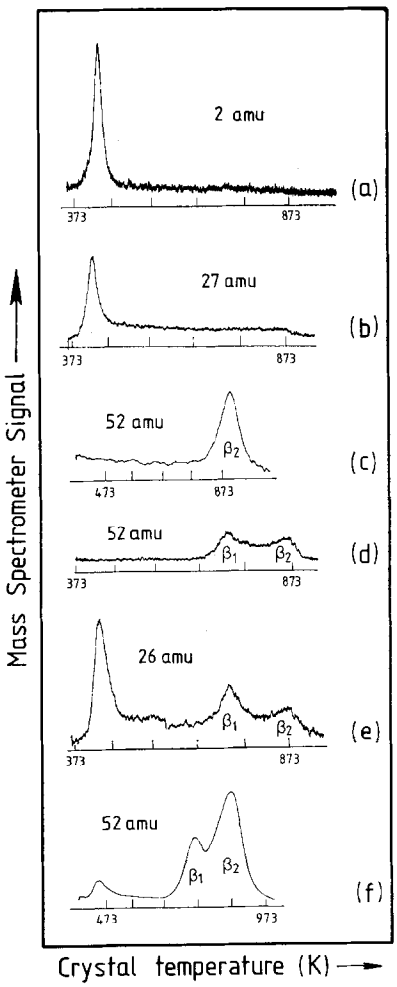

FIG. 1. Thermal desorption spectra: (a)–(e) from Pt(110)–HCN; (f) from Pt(110)–C_2N_2. Heating rate 13 K s^{-1}.

experiments showed that the mass spectrometer filament itself synthesized significant amounts of H_2 from HCN. Since the Pt–H_2 and Pt–HCN desorption spectra overlap strongly, distortion of the former by the pressure burst from the latter vitiates the 2 amu spectra as a reliable measure of the true H_2 yield from the Pt surface. Fortunately, this problem can be circumvented by using the 26 amu spectra for which such difficulties do not arise. These spectra monitor the yields of *both* HCN and C_2N_2, and since there are no other products besides H_2, stoichiometry demands that the H_2 yield be equal to that of C_2N_2. Figure 2a shows the relative yields of C_2N_2 and HCN as well as the total product yield as a function of HCN exposure at 300 K. In deriving these curves from the data, account was taken of the different total ionization cross sections of HCN and C_2N_2 (to correct for gauge sensitivity) as well as the different fragmentation patterns of the two species (which were determined in control experiments). In actual fact, the total ionization cross section of C_2N_2 itself has not been determined: instead, we have used the value (*7*) for butadiene which is likely to be an overestimate of the true value. Figure 2a shows that at low initial coverages the adlayer desorbs entirely as H_2 and C_2N_2, there being no detectable desorption of HCN at coverages up to $\sim 20\%$ of the maximum value. Figure 2b shows the relative sticking probability (S/S_0) of HCN, normalized to the zero coverage value, as a function of total coverage. This curve has been derived from total yield data such as those in Fig. 2a.

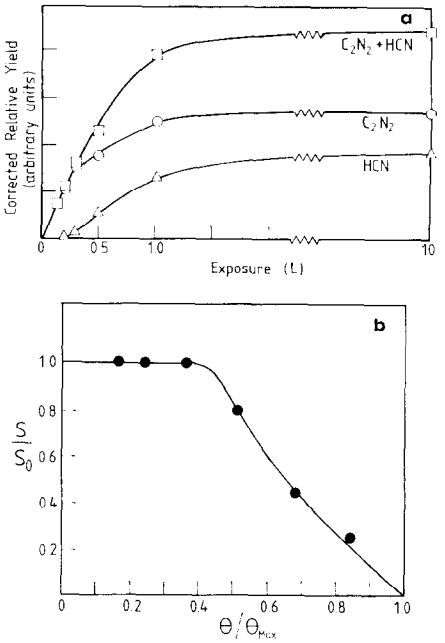

FIG. 2a. Product yields as a function of exposure; (b) relative sticking probability as a function of coverage.

B. LEED and Auger Spectroscopy

The Auger spectrum of an HCN saturated Pt(110) surface was very similar to that already reported (*8*) for a C_2N_2 saturated surface. The carbon and nitrogen KLL transitions appeared with approximately equal intensity, and there were on detectable electron impact effects, again in common with the Pt(110)–C_2N_2 system. The clean Pt(110) surface is reconstructed (1×2), and the LEED pattern from this surface is shown in Fig. 3a. Exposure of this surface at 300 K to HCN resulted in streaking of the diffraction pattern in the [001] azimuth after a dose of 5 L (1 L = 1 Langmuir = 10^{-6} Torr sec); further exposure caused no significant changes in this LEED pattern which is shown in Fig. 3b. On the other hand, exposure of the clean surface to 3 L HCN followed by heating to 530 K (which removes all surface hydrogen either as H_2 or HCN) and annealing at 480 K for 5 min, resulted in the diffuse diffraction pattern shown in Fig. 3c. The unit mesh of the corresponding direct lattice cannot be indexed in terms of Wood's notation (*9*) and is best described by the matrix

$$\begin{vmatrix} 1 & \frac{2}{3} \\ -1 & \frac{2}{3} \end{vmatrix}$$

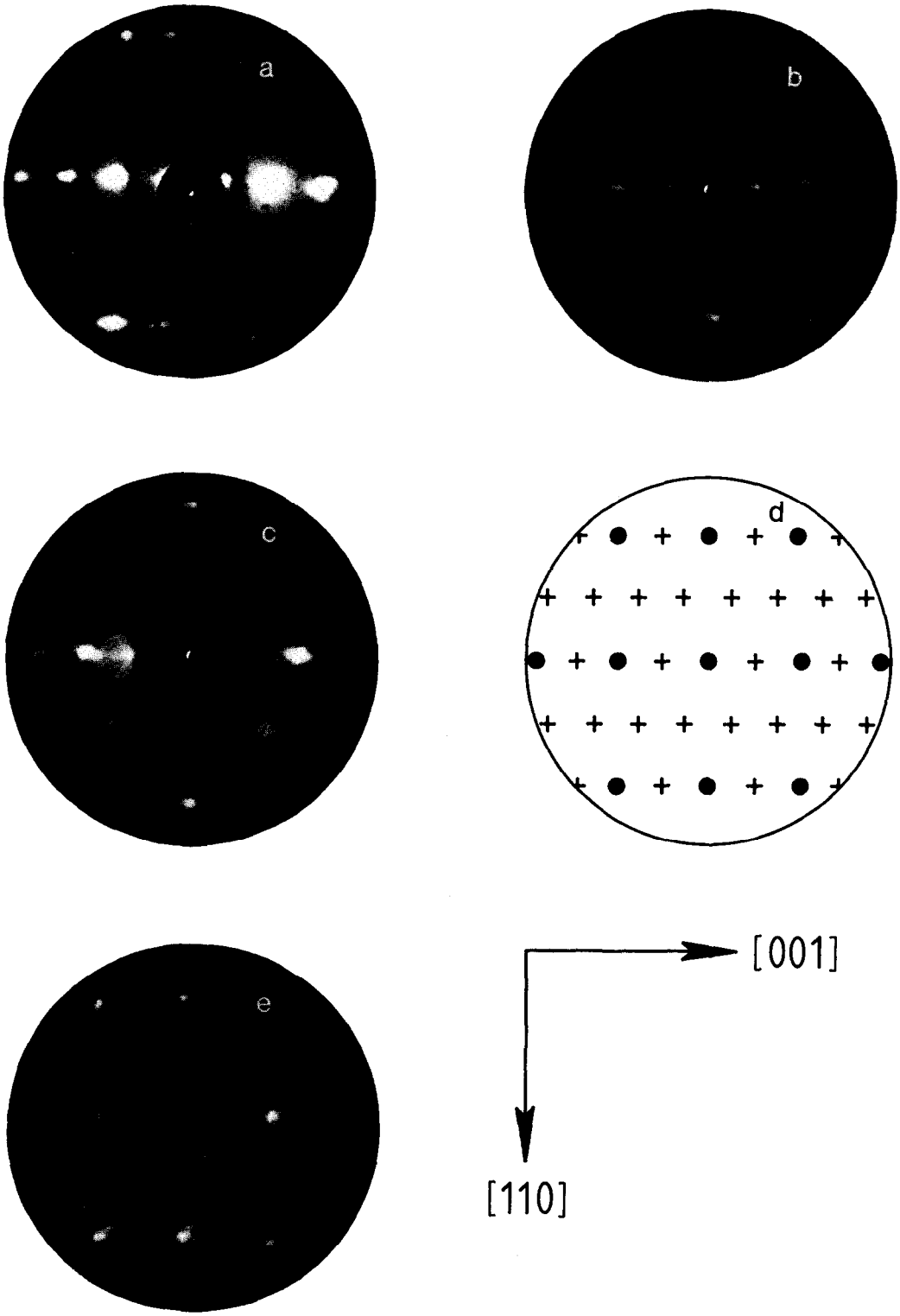

FIG. 3. LEED patterns. (a) clean surface, 54 V; (b) after exposure to 10 L HCN, 75 V; (c) $|1\frac{2}{3}, \bar{1}\frac{2}{3}|$ structure, 75 V; (d) drawing of pattern from $c(2 \times 4)$ structure. (1×1) substrate beams, additional beams due to overlayer; (e) CN saturated surface, 81 V.

which transforms the unit mesh vectors of the solid to those of the overlayer. We will adopt the condensed notation $|1\frac{2}{3},\bar{1}\frac{2}{3}|$ as a convenient way of designating this structure. A further dose of 5 L HCN, followed by the same heating and annealing procedure as already described, results in another diffuse diffraction pattern which corresponds to a $c(2 \times 4)$ surface structure. A schematic representation of this LEED pattern is given in Fig. 3d; the actual photograph has been omitted because it contains a large number of weak and diffuse beams which cannot be reproduced satisfactorily. Dosing the poorly ordered $c(2 \times 4)$ adlayer with a further 10 L of HCN, followed again by heating and annealing procedures, results in the (1×1) pattern of Fig. 3e. No further changes in this LEED pattern could be induced by repeated dosing and heating procedures, and the desorption spectrum of this adlayer shows only the β_1 and β_2 C_2N_2 peaks, as would be expected.

DISCUSSION

The adsorption kinetics of HCN (Fig. 2b) are characteristic of systems in which the chemisorbed state is populated via a weakly bound precursor state which can sample more than one adsorption site. As adsorption proceeds, the surface periodicity along [001] begins to change from that characteristic of the (1×2) surface to that of the (1×1) surface. This behavior has already been observed (*5*, *6*, *8*, *10*) on Pt(110) for all of the species CO, NO, C_2N_2, and C_3O_3. In the cases of CO and NO, no peculiarities are observed in the adsorption kinetics as the periodicity change proceeds. However, with C_2N_2 and C_3O_2, the molecular dimensions are comparable with the periodicity along [001] and the sticking probability *rises* as the $(1 \times 2) \rightarrow (1 \times 1)$ transformation progresses; the effect is quite small in the case of C_2N_2, and most pronounced in the case of C_3O_2. HCN falls in the middle of this series of linear adsorbates, and indeed its adsorption behavior fits the pattern as expected, there being no detectable initial rise in the coverage dependence of the sticking probability.

We have already reported (*8*) a detailed experimental and theoretical study of the desorption of C_2N_2 from adlayers produced by dosing Pt(110) with C_2N_2 itself. In this work, it was concluded that (i) the α peak in the C_2N_2 desorption spectrum was due to the presence of molecularly (i.e., nondissociatively) adsorbed C_2N_2, (ii) the β_1 and β_2 peaks were due to the associative desorption of pairs of CN radicals, with a repulsive energy of $\sim$13.2 kJ mol^{-1} between CN radicals or near-neighbor sites, (iii) a two-dimensional, anisotropic, Monte Carlo calculation showed that associative desorption was only significant for near neighbors along *one preferred direction*. The problem could therefore be treated one-dimensionally, using analytical statistical mechanics.

Before proceeding further, it is necessary to define carefully certain quantities. θ_x refers to the fractional coverage of species x relative to the number of Pt surface atoms in the (1×1)–(110) surface. Θ_x refers to the fractional coverage of x relative to the maximum possible saturation coverage. That is, if x is an adsorbate which occupies n lattice sites, then $n\theta_x = \Theta_x$; Θ_x is the really significant quantity when discussing the statistical mechanics of adsorption layers. Our model for the reactive behavior of the adlayer formed by HCN adsorption is then as follows. Either upon adsorption at 300 K, or when the surface temperature is subsequently raised, HCN surface dissociates, yielding adsorbed H atoms and CN radicals. As the temperature is raised still further, reaction commences in the adlayer with H–H, CN–CN and H–CN recombination reactions occurring, resulting in the desorption of the corresponding molecules. This view is entirely consistent with the complete absence of α C_2N_2, which calls for the presence of

preexisting C_2N_2 molecules in the adsorption layer, as well as the complex coverage dependence of the β_1 and β_2 C_2N_2 peaks. It remains to be shown, given their relatively simpler desorption behavior, that the H_2 and HCN arise in the manner which has been suggested. Direct experimental evidence relating to HCN comes from observations on adlayers made by coadsorbing H_2 and C_2N_2 (*8*). HCN is observed to desorb from such a surface, yielding spectra identical with those in the present work. This strongly supports our suggestion that HCN desorption is the result of H + CN recombination, rather than simple desorption of molecularly adsorbed HCN.

It still remains to be shown that the pseudo-first order appearance of the H_2 and HCN desorption spectra can be accounted for in these terms. We have attempted to do this by setting up the desorption problem as an exercise in two-dimensional lattice statistics, following methods which are already well established (*11*, *12*). The input parameters required to calculate the instantaneous desorption rates at any coverage and temperature are the desorption enthalpies of H_2, HCN and C_2N_2, the preexponential factors for the corresponding desorption reactions, and the interaction energies between nearest-neighbor adsorbate particles. All three quantities for C_2N_2 have already been determined by us (*8*) in our earlier studies of C_2N_2 adsorption. The desorption enthalpy for H_2 from Pt(110) is also known (*13*), and a value for HCN can be estimated from an Arrhenius plot using the 27 amu desorption spectra. Theoretical desorption spectra calculated in this way, for a number of different initial coverages, are shown in Fig. 4. It can be seen that, according to this model, for the case of reactive desorption from an adlayer of H + CN, all three possible products should be observed. This is by no means always the case; thus, for an N + O adlayer, the model predicts (in agreement with experiment) desorption of N_2 and O_2 but no NO (*14*). Physically, the outcome is very largely determined by the relative bond strengths of the desorbing species; in the present case the H–C and H–H bond energies are comparable, so that desorption of the cross product (HCN) can compete effectively with the H_2 forming reaction before the adlayer becomes denuded of H. The results illustrated in Fig. 4 were carried out with an assumed repulsive interaction of 13.2 kJ mol^{-1} between CN–CN near neighbors (*8*), and no interaction between H–H and H–CN pairs. The remaining desorption parameters are specified in Fig. 4. The large preexponential factor for C_2N_2 desorption corresponds to a transition state with one more translational and one more rotational degree of freedom than the reactants. It can be seen that the model gives a very good account of the temperature regimes for desorption of H_2, HCN, and C_2N_2, and that the coverage dependence of the β_2 C_2N_2 peak is well reproduced. The β_1 C_2N_2 peak does not appear, even at maximum coverage ($\theta_H = \Theta_H = \theta_{CN} = \Theta_{CN} = 0.5$, $\theta_{H+CN} = 1$) because this peak only appears (*8*, *11*) for $\Theta_{CN} > 0.5$. Our model has assumed that both H and CN are single site adsorbates which

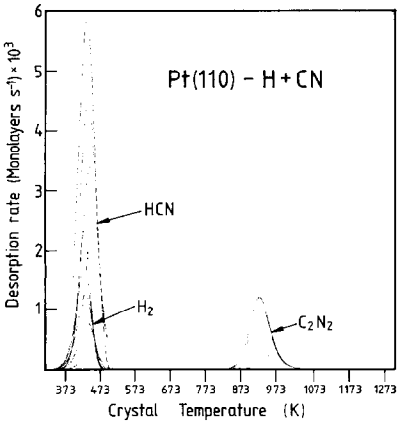

FIG. 4. Calculated spectra for H_2, HCN, and C_2N_2 desorption; preexponential factors 10^{10}, 10^{13}, 10^{23} s^{-1}, respectively, and desorption enthalpies 75, 100, 377 kJ mol^{-1}, respectively.

occupy the same kind of adsorption site (i.e., they compete for sites on a common lattice) so that the maximum initial coverage of CN is $\theta_{CN} = \Theta_{CN} = 0.5$. However, experiment clearly shows that $\Theta_{CN} > 0.5$ does occur, from which we conclude that the H and CN particles must occupy different kinds of site (i.e., they are distributed over two independent sublattices) so that $\Theta_{CN} > 0.5$ is possible. It is therefore clear that our simple 1-lattice model is incorrect, and the 2-lattice problem is analytically intractable. However, our 1-lattice approximation *has* served to illustrate that all the observed major features can be understood in terms of reactive desorption from a fully dissociated adlayer. Furthermore, Fig. 4 also predicts the correct trend for relative product yields, i.e., relatively little HCN to begin with, but eventually an almost constant HCN/C_2N_2 ratio (cf. Fig. 2a). The shape of the H_2 and HCN desorption peaks is in qualitative agreement with experiment, but the predicted coverage dependence of the peak temperatures is somewhat greater than is observed. The agreement could doubtless be improved by adjusting the H–H and H–CN interaction energies, but there would be little point in doing this since the 1-lattice model cannot be strictly correct in any case.

The 52 amu spectrum from a surface dosed with 0.3 L of HCN corresponds very closely to the calculated spectrum (*8*) for $\Theta_{CN} = 0.5$. Furthermore, the β_1 peak is observed for exposures of less than 0.5 L. These facts are understandable only if (i) the absolute value of the initial sticking probability is of order unity and (ii) CN is a two-site adsorbate, i.e., for adsorption at 300 K, the maximum coverage possible corresponds to $\theta_{CN} = 0.5$, $\Theta_{CN} = 1.0$. The saturated surface produced by sequential dosing and thermal treatment, and which is characterized by a (1 × 1) LEED pattern, gives a C_2N_2 desorption spectrum which corresponds to the theoretical spectra (*8*) for $0.6 < \Theta_{CN} < 0.7$. The $c(2 \times 4)$

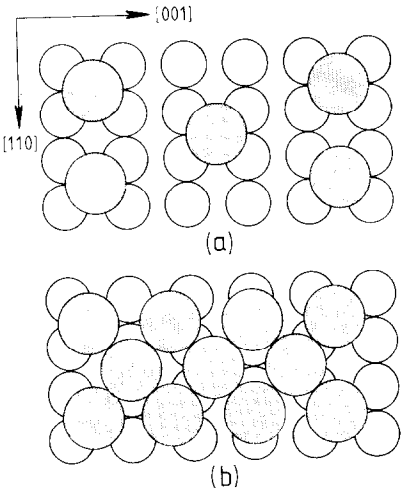

FIG. 5a. $c(2 \times 4)$ structure; (b) $|1\frac{2}{3},\bar{1}\frac{2}{3}|$ structure. (○) = Pt; shaded circles = CN.

structure which precedes the (1 × 1) phase may correspond to either $\Theta_{CN} = 0.5$, $\theta_{CN} = 0.25$, or $\Theta_{CN} = 1.5$, $\theta_{CN} = 0.75$. The second possibility may be ruled out on the grounds that it is *more* concentrated than the (1 × 1) structure and that it requires the unreasonably small separation of 2.77 Å between (see below) some neighboring CN species. The first possibility is illustrated in Fig. 5a; a value of 3.8 Å has been chosen for the effective diameter of adsorbed CN by comparison with (*15*) known structures. This value is also in accord with the effective diameter of chemisorbed CO determined from LEED studies (*16*). Thus far, the LEED and desorption data appear to be consistent with our model. A difficulty arises when one considers the $|1\frac{2}{3},\bar{1}\frac{2}{3}|$ structure which precedes both the $c(2 \times 4)$ and (1 × 1) structures in the formation sequence. The only way to generate a suitable overlayer mesh would appear to be that which is illustrated in Fig. 5b for one particular registry between adsorbate and substrate. This corresponds to $\theta_{CN} = 0.75$, $\Theta_{CN} = 1.5$.

Although it may not be unreasonable that a coverage greater than the room temperature saturation value can be formed

by a dosing–heating–dosing sequence, the problem is that this rather dense structure is observed before the more dilute $c(2 \times 4)$. Inspection of the LEED pattern from the $|1\frac{2}{3},\bar{1}\frac{2}{3}|$ structure (Fig. 3c) shows that the Pt fractional order beams are still visible. The explanation may therefore be that the *average* surface coverage is fairly low, with patches of the dense $|1\frac{2}{3},\bar{1}\frac{2}{3}|$ structure on an otherwise almost bare Pt surface (which would give rise to the fractional order beams). It is interesting to note that (i) the arrangement of the CN species in this structure is similar to the well-established (2×1) *p1g1* structure (*6*, *16*) formed by CO on this surface, (ii) the CN–CN nearest-neighbor spacing is 3.8 Å, and (iii) the $c(2 \times 4)$ structure can be obtained from the $|1\frac{2}{3},\bar{1}\frac{2}{3}|$ structure by removing two out of every three CN rows along [110].

ACKNOWLEDGMENT

M. E. B. thanks the Science Research Council for financial support.

REFERENCES

1. Bond, G. C., "Catalysis by Metals," Chap. 20. Academic Press, New York, 1962.
2. Hucknall, D. J., "Selective Oxidation of Hydrocarbons," Chap. 3. Academic Press, New York, 1974.
3. Lambert, R. M., and Comrie, C. M., *Surface Sci.* **38**, 197 (1973).
4. Lambert, R. M., and Comrie, C. M., *Surface Sci.* **46**, 61 (1974).
5. Comrie, C. M., and Lambert, R. M., *Chem. Soc. Faraday I* **72**, 1659 (1976).
6. Comrie, C. M., Weinberg, W. H., and Lambert, R. M., *Surface Sci.* **57**, 619 (1976).
7. Brown, S. C., "Basic Data of Plasma Physics." M.I.T. Press, Cambridge, Mass., 1967.
8. Bridge, M. E., and Lambert, R. M. *in* IV International Symposium on the Physics and Chemistry of Surfaces (Eindhoven 1976).
9. Wood, E. A., *J. Appl. Phys.* **35**, 1306 (1964).
10. Reed, P. D., and Lambert, R. M., *Surface Sci.* **57**, 485 (1976).
11. Goymour, C. G., and King, D. A., *Chem. Soc. Faraday I* **69**, 749 (1973).
12. Fowler, R., and Guggenheim, E. A., "Statistical Thermodynamics," Chap. 10, Cambridge Univ. Press, London, 1952.
13. Comrie, C. M., PhD thesis, Cambridge, 1973.
14. Bridge, M. E., and Lambert, R. M., unpublished data.
15. Wells, A. F., "Structural Inorganic Chemistry," Chap. 20. Oxford Univ. Press, London, 1962.
16. Lambert, R. M., *Surface Sci.* **49**, 325 (1975).
17. Netzer, F. P., *Surface Sci.* **52**, 715 (1975).
18. Netzer, F. P., personal communication.